

1
2
3
4
5
6
7
8
9
10
11
12
13
14
15
16
17
18
19
20
21
22
23
24
25
26
27
28
29
30
31

**The Hox gene *Antennapedia* regulates wing development through
20-hydroxyecdysone in insect**

Chunyan Fang¹, Yaqun Xin¹, Tao Sun¹, Antónia Monteiro^{2,3}, Zhanfeng Ye¹, Fangyin
Dai¹, Cheng Lu¹, Xiaoling Tong^{1*}

¹ State Key Laboratory of Silkworm Genome Biology, Key Laboratory of Sericultural
Biology and Genetic Breeding, Ministry of Agriculture and Rural Affairs, Southwest
University, Chongqing 400715, China

² Department of Biological Sciences, National University of Singapore, 14 Sciences
Drive 4, Singapore

³ Science Division, Yale-NUS College, 10 College Avenue West, Singapore

* Corresponding author
E-mail: xlton@swu.edu.cn (XT)

32 Abstract

33 A long-standing view in the field of evo-devo is that insect forewings develop
34 without any Hox gene input. The Hox gene *Antennapedia* (*Antp*), despite being
35 expressed in the thoracic segments of insects, has no effect on wing development.
36 This view has been obtained from studies in two main model species, *Drosophila* and
37 *Tribolium*. Here, we show that partial loss of function of *Antp* resulted in reduced and
38 malformed adult wings in *Bombyx*, *Drosophila*, and *Tribolium*. *Antp* mediates wing
39 growth in *Bombyx* by directly regulating the ecdysteroid biosynthesis enzyme gene
40 (*shade*) in the wing tissue, which leads to local production of the growth hormone 20E.
41 In turn, 20E signaling also up-regulates *Antp*. Additional targets of *Antp* are wing
42 cuticular protein genes *CPG24*, *CPH28*, and *CPG9*, essential for wing development.
43 We propose, thus, that insect wing development occurs in an *Antp*-dependent manner.
44 **Key words:** Hox, *Antennapedia*, *shade*, 20E, cuticular protein gene, wing
45 development

46 Introduction

47 The Hox genes encode a family of transcriptional regulators that are important in
48 differentiating the bodies of bilaterian animals along their antero-posterior axis [1].
49 Disruptions to individual Hox genes often leads to disruptions of traits that develop in
50 the regions where the Hox gene is expressed [1].

51 In holometabolous insects, the Hox gene *Antennapedia* (*Antp*) is expressed in all
52 thoracic segments, including in the forewing and hindwing yet, no function has been
53 attributed to this gene regarding wing morphogenesis. In *Drosophila*, wing and haltere
54 primordia could be detected in embryos even in the complete absence of *Antp*
55 function in homozygous mutants of *Antp* [2]. In addition, a very low level of *Antp*
56 protein present in the growing wing imaginal disc, suggested that forewing formation
57 did not require *Antp* [2]. Similarly, no obvious phenotypes were observed in adult
58 *Tribolium* elytra (forewing) or hindwing after RNA interference (RNAi) of *Antp*.
59 These data suggested that wing development takes place without any *Antp* input [3].
60 In contrast, the Hox gene *Ultrabithorax* (*Ubx*), expressed exclusively in hindwings,
61 functions to differentiate hindwings from forewings. Forewing development in insects
62 was, thus, thought to occur without any significant Hox gene input [3-13].

63 Recently, however, we observed that two loss of function mutations in the silkworm
64 *Bombyx mori Antp* gene (*BmAntp*), *Nc* and *Wes*, displayed abnormal wings [14,15].
65 These mutations had not been examined beyond the embryonic stage due to lethality,
66 but could be maintained in heterozygous lines. The adults of these lines displayed
67 reduced and malformed wings.

68 These two *Bombyx Antp* mutants, however, shared common features with
69 *Drosophila Antp* mutants, observable in embryos. The homozygous (*Antp*^{-/-}) embryos
70 died late in embryogenesis but displayed a homeotic transformation of thoracic legs to
71 antenna-like appendages[14-17]. The novel wing phenotypes in *Bombyx* heterozygote
72 mutants, however, suggested that *Antp* was affecting wing development, a role not

73 previously documented for this gene because embryos died long before the stage
74 when wings start to develop. In the present study, we used wildtype and heterozygotes
75 of the *Wes* strain (*Antp*^{+/-}) as the study objects to more fully understand the role of
76 *Antp* in wing development.

77 Results

78 *BmAntp* is involved in the development of wings in *Bombyx*

79 Since defective adult wings were observed in aberrant *Antp* *Wes* and *Nc* mutants
80 (*Antp*^{+/-}) [14,15], we sought to test when in development *Antp* input was required. We
81 analyzed the expression profile of *BmAntp* in the forewing and hindwing of wildtype
82 (WT) individuals from the 3rd day of the 5th instar to the adult stage. qRT-PCR
83 revealed that the expression of *BmAntp* was maintained at a low level in the larval
84 stage and gradually increased and reached a peak on the 6th day of the pupal stage.
85 Forewings expressed higher levels of *Antp* relative to hindwings at most times during
86 the pupal stage (Fig 1A). Then, we compared the expression pattern of *BmAntp*
87 between mutant *Wes* (*Antp*^{+/-}) and WT individuals. *BmAntp* was expressed at a
88 consistent but lower level in the mutants compared to WT controls (Fig 1B).

89 To evaluate the effects of *BmAntp* expression levels on wing morphology during
90 development, we dissected the wing discs of *Wes* (*Antp*^{+/-}) and WT from the 3rd day of
91 the last larval instar to the wandering stage larva. Wing disc size increased slowly
92 during the larval stage and was not significantly different between *Wes* mutants
93 (*Antp*^{+/-}) and WT individuals. Then, during the wandering stage, the wing morphology
94 changed dramatically. The wing discs of *Wes* mutants (*Antp*^{+/-}) were curlier and
95 smaller than those of WT, and finally degenerated to tiny and wrinkled adult wings
96 (Fig 1C).

97 To confirm the function of *BmAntp* in wing development, we performed RNAi
98 injections into WT larvae of *B. mori*. We synthesized dsRNA targeting *BmAntp* and
99 injected it into larvae on the 1st day of the wandering stage. qRT-PCR showed that
100 *BmAntp* dsRNA efficiently reduced *BmAntp* transcript levels compared to controls
101 injected with *EGFP* dsRNA (Fig 1D). Nineteen out of 22 (86%) *BmAntp* dsRNA
102 treated individuals had small wings similar to the *Wes* mutant (*Antp*^{+/-}) while control
103 silkworm adults grew their wings normally (Fig 1E).

104 To further confirm the function of *BmAntp* we performed crisper-Cas9 injections
105 into WT embryos of *B. mori*. We generated a genomic disruption of the *BmAntp* gene
106 by targeting its first exon using four specific single-guide RNAs (sgRNAs) and the
107 Cas9/gRNA ribonucleoprotein (RNP) delivery system (Fig 1F). After injection, 20
108 eggs hatched and 18 larvae developed to the adult stage. We found that 61% of the
109 moths (11 individuals) displayed malformed adult wings (S2 Table, Fig 1G), and
110 confirmed that various insertions and deletions were present at the location targeted
111 by the four sgRNAs (Fig 1H). Abnormal wings were not observed in control
112 injections with *BmBLOS2* sgRNA which only led to translucent larval skin. These
113 data indicate that *BmAntp* is a critical transcription factor that regulates wing
114 development in *B. mori*.

115 **BmAntp affects the synthesis of 20E by regulating the expression of *Shade* in**
116 **wing discs**

117 We next tested whether the production of abnormal wings in *BmAntp* mutants was
118 related to deficits in levels of the molting hormone, 20-hydroxyecdysone (20E). We
119 tested this hypothesis because 1) Significant differences in the size of wing discs were
120 observed between *BmAntp* mutants and controls starting from the onset of the
121 larva-to-pupa transition (Fig 1C); 2) A pulse of this steroid hormone normally
122 regulates the larva-to-pupa transition; and 3) 20E is a major regulator of wing growth
123 and development [16, 17].

124 We first examined the expression level of genes involved in the ecdysteroid
125 biosynthesis pathway in a variety of tissues. We found that *spookier*, *phantom*,
126 *disembodied*, and *shadow* were expressed in the prothoracic gland (PG), as expected,
127 as this is the main source of ecdysteroid synthesis in insect larvae [5]. In addition, the
128 *shade* gene, which codes for a P450 monooxygenase that catalyze ecdysone into the
129 active 20E in targeted peripheral tissues [18], was primarily expressed in the wing
130 discs compared to the PG and hemolymph (Figs 2A–2E).

131 We next explored whether *Wes* mutants (*Antp*^{+/-}) expressed *shade* at different levels
132 relative to WT wings, and whether this impacted levels of 20E in the wing tissue. The
133 *shade* transcripts were present at markedly higher levels in WT than in *Wes* mutant
134 (*Antp*^{+/-}) wings, and levels reached a peak on the 4th day of the pupal stage (Fig 2F).
135 Titers of ecdysone measured from wing discs on that day (P4), were similar between
136 *Wes* mutants (*Antp*^{+/-}) and WT individuals. Titers of 20E, however, were significantly
137 lower in *Wes* mutants (*Antp*^{+/-}) relative to WT individuals two days later (on P6) (Figs
138 2G and 2G’).

139 We next investigated whether the expression levels of *Ecdysone Receptor (EcR)*
140 and *ultraspiracle (usp)* [19], the receptors that bind 20E to transduce edysone
141 signaling to the nucleus were also different between *Wes* and WT individuals. This is
142 because 20E signaling is known to up-regulate expression of *EcR* and *usp* in the
143 wings of *Drosophila* [20,21]. Significantly lower levels of *usp*, and of the two
144 isoforms of *EcR*, *EcRA* and *EcRB* mRNA were detected in the mutants compared with
145 WT on day P4 (S1 Fig). These results suggest that *Antp* is also regulating the
146 expression of these genes, either directly or indirectly. The latter mechanism could
147 involve *Antp* up-regulating *shade*, which increases 20E titers in the wing cells which,
148 in turn, up-regulates *EcR* and *usp* transcription in wings.

149 We next sought to test whether *shade* was a direct target of *BmAntp*. We examined
150 a 2 kb region of DNA immediately 5’ of the start site of *shade* for possible *Antp*
151 binding domains and found a total of five such domains (Figs 2H and 2H’). To
152 evaluate the extent that DNA containing one or more of these domains could regulate
153 flanking gene expression we cloned different sized fragments, containing a different
154 number of *Antp* binding domains, upstream of the reporter gene *luciferase*. We
155 transfected this plasmid into *BmN* cells and co-transfected *BmAntp* in these cells as
156 well (S2 Fig). The largest fragment (-1985 to -300), containing all five *Antp* binding
157 sites, led to significantly increased luciferase activity compared to the other four
158 fragments (Fig 2I). These data suggest either that a regulatory region -1985 to -1470

159 containing a key Antp binding site or, more likely, that all Antp sites together are
160 required for the transcriptional regulation of *shade*, and that *shade* is likely a direct
161 target of BmAntp.

162 To determine whether BmAntp protein could directly bind to the *in silico* identified
163 Antp binding sites of the *shade* promoter, we designed a specific biotinylated probe
164 covering the -1985 to -1470 genomic region of *shade* and conducted electrophoretic
165 mobility shift assay (EMSA) (Fig 2J). We further validated the direct regulation of
166 BmAntp on Shade transcription through *in vivo* ChIP-PCR following the BmN cells
167 which were overexpression of *FLAG*-tagged *BmAntp* (Fig 2K, S3 Fig). Our data
168 indicated that BmAntp activates the transcription of *shade* by directly binding to the
169 tested genomic region.

170 ***BmAntp* is upregulated by 20E**

171 We next sought to investigate which genes could be driving *Antp* expression in the
172 wings of *B.mori*. *Antp* levels were low throughout wing disc development until the
173 pupal stage, and then followed a slow rise and fall. Because this expression profile
174 resembled the 20E titer profile in *B.mori* hemolymph [22], we decided to investigate
175 whether the 20E/EcR/USP complex could be upregulating *Antp* in pupal wings. We
176 first examined potential Ecdysone Response Element (EcRE) binding sites for the
177 complex within the ~2 kb upstream of *BmAntp* (counting from the start codon of 5'
178 UTR) and discovered three such sites (EcRE1, -139– -153 nt; EcRE2, -1034– -1048 nt;
179 EcRE3, -1592– -1606 nt) (Fig 3A). Then, we cloned this ~2kb genomic region of
180 *BmAntp* in front of the luciferase reporter gene and transfected this plasmid into BmN
181 cells, followed by 20E treatment. Subsequent dual luciferase reporter assays revealed
182 that this region drove significantly higher luciferase activity after 20E application (Fig
183 3B). To further confirm the upregulation of *BmAntp* expression by 20E, we used
184 qRT-PCR to show that the expression of *BmAntp* was significantly upregulated both
185 in cultured cells and in wing discs after 20E treatment (Figs 3C and 3D). These data
186 show that 20E can upregulate expression of *BmAntp* via the direct binding of the
187 20E/EcR/USP complex to a 5' upstream region of the gene.

188 **BmAntp directly regulates wing-specific cuticular protein genes**

189 In order to explore potential additional targets of Antp, besides *shade*, that might
190 have contributed to the small wings of adult *Wes* mutants, we investigated the
191 expression of four cuticular proteins with a known expression profile, that matched
192 that of *Antp*, in both WT and *Wes* mutants. In particular, expression levels of *CPH28*,
193 *CPG24*, *CPG9* peaked at P5, as did expression of Antp (Fig 1B) [20]. *CPG11*, by
194 contrast, was expressed primarily during the early 5th instar, and was used as a control
195 gene [23]. Previous work has shown that cuticular proteins are major components of
196 insect wings and that both EcR-mediated signaling as well as other transcription
197 factors regulate their very dynamic and specific expression profiles [24-26]. qRT-PCR
198 analysis showed that the expression levels of *CPH28*, *CPG24*, *CPG9*, and *CPG11* in
199 *Wes* (*Antp*^{+/-}) were remarkably lower than those of WT (Fig 4A). We explored the
200 direct regulation of these four cuticular proteins by Antp by conducting Luciferase

201 reporter assays in BmN cells with candidate genomic regions (3kb upstream of each
202 gene) containing putative Antp binding sites (Fig 4B). Increasing *BmAntp* levels in
203 these cells significantly upregulated the transcription of *CPH28*, *CPG24*, and *CPG9*
204 (Figs 4C–4F), but not *CPG11*. A dual-Luciferase assay with *CPH28* further showed
205 that BmAntp can directly elevate the expression of *CPH28* (Fig 4G). Moreover, an
206 EMSA and ChIP-PCR assay showed that BmAntp was able to directly bind the *in*
207 *silico* identified Antp binding sites in the *CPH28* promoter (Figs 4H and 4I, S4 Fig).
208 These results indicate that BmAntp can upregulate the transcription of these three
209 wing cuticular protein genes, and *CPH28* is likely up-regulated by a direct interaction
210 of Antp with this gene's promoter.

211 To determine whether *CPH28* is essential for wing development, we knocked it
212 down using RNAi. *CPH28*-siRNA was injected into 18 pupae, and the same quantity
213 of scrambled siRNA sequence was injected in control animals. Levels of *CPH28*
214 decreased significantly in the wing discs 48 h after *CPH28*-siRNA injections relative
215 to control injections (Fig 4J). The ratio of malformed wings reached 80% after
216 eclosion (Fig 4K, S3 Table). In contrast, all moths in the control group had normal
217 wings (Fig 4K). These results indicate that *CPH28* is required for the generation of
218 normal wings in silkworms.

219 ***Antp* function in wing development is conserved in *Drosophila* and *Tribolium***

220 To evaluate whether the function of *Antp* in wing development is conserved across
221 other insect orders, we examined the wings of adult flies and beetles after *Antp*
222 down-regulation. In *Drosophila* we drove expression of *Antp* RNAi hairpins in larval
223 and pupal wing discs under the control of the *nubbin-gal4* (*nub-gal4*) driver. All
224 individuals in which *Antp* was knocked down had rudimentary wings that were
225 reduced in size compared to controls (Figs 5A–5D). In *Tribolium*, we injected *Antp/ptl*
226 dsRNA during the last larval stage, just before the onset of rapid wing growth [3].
227 These injections led to lower mRNA levels of *Antp/ptl* (S5A Fig) and to wrinkled and
228 shortened forewings (elytra) and hindwings (Figs 5E–J, S5B and S5C Figs).
229 Additionally, the uniform mesonotum phenotype observed in the *Antp/ptl* RNAi adults
230 was consistent with that reported by Tomoyasu and colleagues (Figs 5K and 5L, S5D
231 and S5E Figs) [3]. These observations indicate that *Antp* plays a crucial role in the
232 development of wings in *Drosophila* and *Tribolium*. Taken together, these results
233 demonstrate that *Antp* participates in insect wing development in a conserved manner.

234 **Discussion**

235 **Hox gene *Antp* is indispensable for wing development**

236 Limited experiments in previous *Drosophila* studies, focusing on embryonic and
237 larval stages, likely prevented the identification of *Antp*'s role in later stages of wing
238 development. Fly embryos homozygous for *Antp*^{W10}, a mutation in the *Antp* sequence,
239 led to normal wing primordia, whereas ectopic expression of *Antp* in third instar larval
240 wing discs had no effect on larval wing discs morphology [2]. This lack of results is
241 expected as *Antp* protein was largely absent in the major region of the growing larval

242 discs [2]. In the present study, the *nub-Gal4* driver was used to drive *UAS-Antp^{RNAi}*
243 expression in fly wing discs. We chose this driver as its expression was first detected
244 in late 2nd instar wing discs and persisted through late pupal wings [27]. This led to a
245 prolonged silencing of *Antp* expression and to malformed adult wings in *Drosophila*.
246 Given that the silkworm *Antp* was also expressed at low levels in larval wings, but at
247 much higher levels in pupal wings, we speculate that there is no requirement for *Antp*
248 function during the embryo and larval stages, but *Antp* is important for wing
249 development in the later pupal stages.

250 Our RNAi experiment in *Tribolium castaneum* also identified strong wing defects
251 not previously identified with a previous similar RNAi experiment [3]. This previous
252 study only reported variation of mesonotum morphology [3], which was also found in
253 our experiment. We performed the *Antp* RNAi experiment twice (>250 individuals)
254 and obtained consistent defective wing morphologies, that were not observed in
255 control animals injected with dsRNA against *EGFP*. We speculate that the different
256 outcomes of the two experiments may be due to the different ds*Antp* fragments used.
257 We used two fragments covering a larger region of the *Antp* gene (922bp) compared
258 to the 535 bp fragment used by Tomoyasu et al.. Based on the present results, we
259 propose that *Antp* is necessary for wing development in *Bombyx*, *Drosophila*, and
260 *Tribolium*.

261 Recently, *Antp* input was found to be required for the development of two novel
262 traits in the wings of the nymphalid butterfly *Bicyclus anynana*: silver scales and
263 eyespot patterns, in both forewings and hindwings, but only minor wing growth
264 deformities were reported (see Fig 2B in Matsuoka and Monteiro) [28]. It is possible
265 that the role of *Antp* has shifted from a general wing growth role to a more specialized
266 role in color pattern formation. This might be the case in this species and other
267 nymphalids where *Antp* expression has been visualized in the eyespots [27,29].
268 Alternatively, the mosaic disruptions obtained with this crispr-Cas9 experiment were
269 insufficient to uncover a more general role of *Antp* in wing growth and development.
270 Most interestingly, the effect of *Antp* on *shade* expression should be investigated in
271 connection to 20E-mediated eyespot size plasticity in this species [27,29].

272 **Bi-directional regulation between *Antp* and 20E**

273 We showed that *Antp* directly binds to the promoters of *shade*, a gene coding for
274 the last step in the production of the active ecdysteroid, 20E, and that 20E was
275 produced inside wing tissues from the precursor ecdysone produced in the prothoracic
276 gland [25,30]. The biosynthesis of 20E, the main hormonal regulator of molting and
277 metamorphosis in insects [17,31], is mediated by the Halloween genes, such as
278 *spookier*, *shroud*, *disembodied*, *shadow* and *shade* [32]. *shade* is known to convert
279 ecdysone into 20-hydroxyecdysone (20E) in peripheral organs such as the fat body,
280 midgut and Malpighian tubules [25,30]. As expected, the mRNA coding for *Shade*
281 mRNA was present at an extremely low level in the prothoracic gland and also in the
282 hemolymph, but at a higher level in wing discs. Given that the mRNA expression of
283 *shade* in wing discs of *Wes* (*Antp^{+/-}*) mutants was significantly lower than that in
284 normal wing discs, this explains the observed lower levels of 20E, but not of ecdysone,

285 in the wing tissue of these mutants, and associated wing disc growth disruptions.

286 In our study, we also found that supplementary 20E up-regulated *Antp* in both
287 BmN cells and in developing wing discs. Similar regulation of Hox genes by 20E
288 have previously been reported in the *Drosophila* heart, where the expression of *Ubx*
289 and *abdominal-A (abdA)*, was also activated by ecdysone signaling [33]. So, *Antp*
290 upregulates 20E in the wing, and 20E together with its nuclear co-receptors (EcR and
291 USP) upregulate *Antp*, *EcR* and *usp* expression.

292 ***Antp* regulates the expression of wing cuticular protein genes**

293 Cuticular proteins are major components of insect wings and previous studies had
294 already implicated the regulation of these proteins by other Hox genes. A total of 52
295 cuticular protein genes were detected in silkworm wing discs by expressed sequence
296 tags [23]. The regulation of one these proteins, BmWCP4, was previously shown to
297 be dependent on the co-binding of the Hox gene *BmAbd-A* with the transcription
298 factor *BmPOUM2*, in the gene's promoter [34]. In the present study, we focused on
299 investigating wing cuticular protein genes whose expression patterns were largely
300 congruent with that of *Antp* [31]. We showed that they were remarkably
301 down-regulated in mutant (*Antp*^{+/-}) individuals, and that disruptions to one of these
302 proteins impaired wing development. It remains possible, that many more additional
303 *Antp* targets remain to be described.

304 Previous studies have assumed that the forewing is a Hox-free wing [3,5,9]. Our
305 data indicated that *Antp* is crucial for wing development in insects (Fig 6). It does this
306 by directly enhancing transcription of the steroidogenic enzyme gene *shade* in wings
307 and, thus, controlling the synthesis of an essential growth hormone, 20E, directly in
308 the wing tissue. In turn 20E signaling upregulates *Antp* expression. *Antp* also directly
309 regulates the expression of critical cuticular protein genes in both forewings and
310 hindwings.

311 **Materials and Methods**

312 **Animal Strains.** (1) The wild-type (WT) strain *DaZao* and mutant strain *Wes* (*Antp*^{+/-})
313 were obtained from the Silkworm Gene Bank of Southwest University, China.
314 Silkworms were reared on mulberry leaves at 25°C in ~75% relative humidity with a
315 12:12 h (L:D) photoperiod during their entire life. (2) The following fly stocks were
316 used in this study: The WT *yw* and *nub-gal4* enhancer trap lines (BCF391#) were
317 obtained from Core Facility of Drosophila Resource and Technology. The
318 *UAS-Antp*^{RNAi} (THU2760) was supplied by the Tisng Hua Fly Center. The wildtype *yw*
319 were used as control flies. All individuals were incubated at 25°C. (3) The *Tribolium*
320 *castaneum* *GA-1* strain was used in this study. Insects were reared in whole wheat
321 flour containing 5% brewer's yeast at 30°C under standard conditions.

322

323 **Bombyx cell lines.** The *Bombyx mori* ovary-derived cell line BmN was cultured at
324 27°C in TC-100 medium (United States Biological) supplemented with 10% fetal
325 bovine serum (Gibco) and 2% penicillin/streptomycin (Gibco).

326

327 **RNA Extraction and qRT-PCR.** Total RNA samples were isolated from wing discs,
328 prothoracic glands, hemolymph, BmN cells, and the whole beetles at different time
329 points or under different conditions, using the MicroElute Total RNA kit (Omega) in
330 accordance with manufacturer instructions. The cDNA was synthesized with 1 ug
331 total RNA using the PrimeScriptTM RT Reagent Kit with gDNA Eraser (TaKaRa).
332 qRT-PCR was performed using a qTOWER³G system (analytikjena) and a qPCR
333 SYBR Green Master Mix (Yeasen). The eukaryotic translation initiation factor 4A
334 (BmMDB probe ID sw22934) was used as an internal reference in *Bombyx*, and
335 ribosomal protein S3 (*rps3*) in *Tribolium castaneum*. All experiments were
336 independently performed with three biological replicates and the results were
337 calculated using the 2^{-ΔΔCT} method. Primers are listed in S1 Table.

338

339 **RNAi Experiment in *Bombyx* and *Tribolium*.** The double-strand RNA (dsRNA) of
340 *Antp*, *CPH28*, *ptl1*, *ptl2*, and *EGFP* were synthesized using the RiboMAX Large
341 Scale RNA Production System T7 kit (Promega). Approximately 100 μg of
342 synthesized ds*Antp* was injected into the second chest spiracle at the first day of
343 *Bombyx* larval wandering stage. We injected 0.4–0.5 μg of ds*ptl* at the ratio of 1:1 mix
344 *ptl1* and *ptl2* final instar larvae of *Tribolium castaneum*. To knockdown *CPH28*
345 expression in the silkworm pupal stage, the siRNA sites
346 5'-GCAGCAAUUGUUCGCACAATT-3' and
347 5'-GGAAGCUUUACAUCGGUUTT-3' (GenePharma) for *CPH28* were designed.
348 Ten μl of siRNA 1 μg/μl was injected from the breathing-valve into the wing disc on
349 the 4th day of the pupal stage. In addition, after injection, all insects were reared in a
350 suitable living environment until analysis.

351

352 **Down-regulation of *Antp* in *Drosophila* wings** We used the Gal4/UAS system to

353 knockdown *Antp* gene expression in *Drosophila* wings. We crossed the *UAS-Antp^{RNAi}*
354 males with *nub-gal4* virgin females and then incubated them at 25°C on a
355 yeast/saccharose medium. The wing phenotypes of F1 adults were observed.

356

357 **CRISPR/Cas9-mediated *Antp* Knockout in *Bombyx*.** The sgRNAs for knocking out
358 *Antp* was designed by <http://crispr.dbcls.jp/> and synthesized using the RiboMAXTM
359 Large Scale RNA Production System T7 kit (Promega). Cas9 protein was purchased
360 from Invitrogen (Thermo). The four sgRNAs and the Cas9 protein were mixed at a
361 dose of 500 ng/ul. The mixture was incubated for 15 min at 37°C to produce a
362 ribonucleoprotein complex (RNP) and micro-injected into the silkworm embryos
363 within 2 h post oviposition. The injected embryos were incubated at 25°C and >90%
364 relative humidity until they hatched. Genomic DNA of adult wings was extracted
365 using the DNAzol (Takara) according to the manufacturer protocol. The target region
366 was amplified using site-specific primers (Table S1). PCR products were checked by
367 PAGE gel and sequencing approach. Related promoters are listed in Table S1. These
368 sgRNAs synthesized *in vitro* were mixed with Cas9 protein and micro-injected into
369 preblastoderm embryos of the *DaZao* strain.

370

371 **ELISA.** ELISA was used to calibrate the ecdysteroid titer in wing disc of WT and
372 *Antp* mutants. Silkworm wing discs were collected from ~50 pupae, and the pooled
373 sample homogenized in methanol. The homogenate was centrifuged and we
374 evaporated the supernatant at 55°C. The solid matter remaining was redissolved in 1
375 mL EIA buffer (Cayman Chemical) for 20E measurement and 1 mL sample diluents
376 (BIOHJ) for ecdysone measurement, respectively. Ecdysteroid titers were assayed by
377 an ELISA kit according to manufacturer instructions (Cayman Chemical or BIOHJ).
378 Absorbance was measured at 414 nm for Cayman kit or 450 nm for BIOHJ kit on a
379 BioTek H1 microplate reader.

380

381 **20E Application.** For 20E treatment in *Bombyx* and BmN cells, 20E (Adooq) was
382 dissolved in DMSO and then diluted to the experimental concentrations with
383 deionized distilled water. The final concentration of DMSO was 0.1% (v/v) in water.
384 A total of 4 µg 20E was injected into larvae at the mesothoracic region on the 1st day
385 of the larval wandering stage. An equal volume of DMSO at a final concentration of
386 0.1% (v/v) was used as the control. After 24 h, the wing discs were dissected in TRK
387 lysis buffer (Omega). Five-µm 20E were applied to BmN cells for 24 h and then
388 collected. An equal volume of DMSO was used as the control.

389

390 **Dual Luciferase Assay.** The different lengths of *shade*, *CPH28*, and *Antp* promoters
391 were subcloned into the pGL3-basic vector (Promega). The ORF of red fluorescent
392 protein gene (*RFP*)-fused *Antp* was inserted into a pIZ/V5-His vector (Invitrogen)
393 driven by the OpIE2 promoter. Different truncated promoters of pGL3-basic vector
394 were co-transfected with pIZ/V5-His-*Antp* or treated with 20E at a concentration of 5
395 µM. After approximately 24 or 48 h transient transfection, dual-luciferase activities
396 were measured using the Dual-Glo Luciferase Assay Kit (Promega). A pRL-TK vector

397 containing the Renilla luciferase gene was used as an internal control.

398 **EMSA.** Recombinant Antp nuclear proteins were extracted from *E. coli* strain BL21
399 (DE3) competent cells (TransGen). The potential Antp binding sites of the *shade* and
400 *CPH28* promoters were predicted by the GENOMATIX system
401 (<http://www.genomatix.de/solutions/index.html>) and JASPAR CORE
402 (<http://jaspar.genereg.net/>). The DNA oligonucleotides containing Antp binding sites
403 were labeled with biotin at the 5'-end and annealed to generate probes. EMSA
404 experiments were conducted according to manufacturer instructions for the
405 EMSA/Gel-Shift Kit (Beyotime). The binding reactions were performed with 4 µg
406 recombinant Antp protein and different amounts of biotin-labeled probes (10 pmol, 20
407 pmol, 40 pmol) for 30 min at room temperature. For competition assays, 40 pmol
408 unlabeled competitor probes were added to the reaction mixture. These samples were
409 electrophoresed on 5% polyacrylamide gels in 0.5×TBE at room temperature. The
410 total probes are listed in S1 Table.

411

412 **ChIP Assay.** To further detect the effects of Antp on the activity of the *shade* and
413 *CPH28* promoters, the ChIP assay was performed following kit instructions (GST).
414 BmN cells were transfected with a *Flag-Antp* expression vector and harvested at 48 h.
415 These cells were fixed with 37% formaldehyde, and then DNA containing proteins
416 were sonicated to obtain 200–1000 bp length DNA fragments. The
417 immunoprecipitation reactions were enriched with 1 µg antibody against Flag or IgG.
418 The precipitated DNA and input were used for PCR analysis. The primers used for
419 amplifying the sequences containing potential Antp binding sites are listed in S1
420 Table.

421

422 **Statistical Analysis.** Statistical analyses were performed using GraphPad Prism 7
423 (GraphPad Software). The data are presented as the mean ± standard error (SE). The
424 differences between two sets of data were analyzed with Student's t-test. A value of
425 $P < 0.05$ was considered statistically significant; * $P < 0.05$, ** $P < 0.01$, and *** $P <$
426 0.001.

427 **Acknowledgments**

428 This work was supported by the National Natural Science Foundation of China [No.
429 U20A2058, No. 31830094]. AM acknowledges support from the National Research
430 Foundation Singapore Investigatorship award NRF-NRFI05-2019-0006.

431 **Author contributions**

432 X. T. and C. F. designed the project. C. F., Y. X., and T. S. performed the
433 experiment. C. F., A. M., and X. T. wrote the manuscript.

434 **Competing interests**

435 The authors declare no competing financial interests.

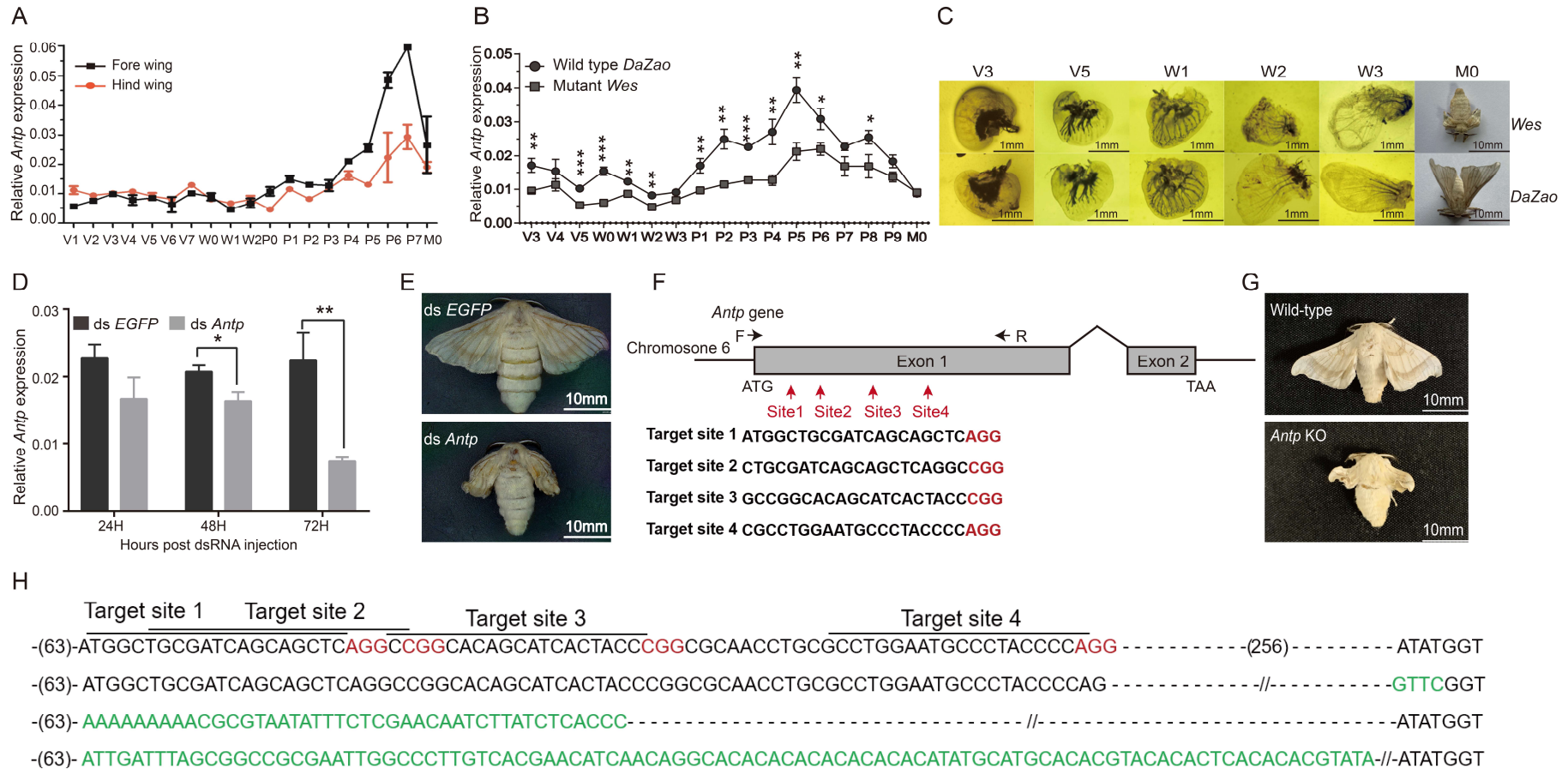
436 **References**

- 437 1. Mallo M, Alonso CR. The regulation of Hox gene expression during animal
438 development. *Development*. 2013;140(19):3951- 63.
- 439 2. Carroll SB, Weatherb Ee SD, Langeland JA. Homeotic genes and the regulation
440 and evolution of insect wingnumber. *Nature*. 1995;375(6526):58-61.
- 441 3. Tomoyasu Y, Wheeler SR, Denell RE. Ultrabithorax is required for membranous
442 wing identity in the beetle *Tribolium castaneum*. *Nature*. 2005;433(7026):643-7.
- 443 4. Deutsch J. Hox and wings. *Bioessays*. 2005;27(7):673–5.
- 444 5. Struhl G. Genes controlling segmental specification in the *Drosophila* thorax.
445 *Proc. Natl. Acad. Sci. USA* 79, 7380-7384. Proceedings of the National Academy of
446 Science. 1983;79(23):7380-4.
- 447 6. Roch F, Akam M. Ultrabithorax and the control of cell morphology in *Drosophila*
448 halteres. *Development*. 2000;127(1):97-107.
- 449 7. Tomoyasu, Yoshinori. Ultrabithorax and the evolution of insect
450 forewing/hindwing differentiation. *Curr. Opin. Insect Sci*. 2017;19, 8-15.
- 451 8. Liu F, Li X, Zhao M, Guo M, Han K, Dong X, et al. Ultrabithorax is a key
452 regulator for the dimorphism of wings, a main cause for the outbreak of planthoppers
453 in rice. *Natl. Sci. Rev.*2020;(7):7.
- 454 9. Weatherbee SD, Halder G, Kim, J, Hudson A, Carroll S. Ultrabithorax regulates
455 genes at several levels of the wing-patterning hierarchy to shape the development of
456 the *Drosophila* haltere. *Genes Dev*. 1998;12(10):1474-82
- 457 10. Weatherbee SD, Nijhout HF, Grunert LW, Halder G, Galant R, Selegue J, et al.
458 Ultrabithorax function in butterfly wings and the evolution of insect wing patterns.
459 *Current Biology Cb*. 1999;9(3):109-15.
- 460 11. Lewis EB. A gene complex controlling segmentation in *Drosophila*. *Nature*. 1978;
461 276(5688):565-70.
- 462 12. Pavlopoulos A, Akam M. Hox gene Ultrabithorax regulates distinct sets of target
463 genes at successive stages of *Drosophila* haltere morphogenesis. *Proc. Natl. Acad. Sci.*
464 *USA*. 2011;108(7):2855-60.
- 465 13. Carroll SB, Weatherb Ee SD, Langeland JA. Homeotic genes and the regulation
466 and evolution of insect wingnumber. *Nature*.1995;375(6526):58-61.
- 467 14. Nagata T, Suzuki Y, Ueno K, Kokubo H, Xu X, Hui C, et al. Developmental
468 expression of the *Bombyx Antennapedia* homologue and homeotic changes in the *Nc*
469 mutant. *Gene cells*. 1996;1(6):555-68.
- 470 15. Chen P, Tong XL, Li DD, Fu MY, He SZ, Hu H, et al. *Antennapedia* is involved
471 in the development of thoracic legs and segmentation in the silkworm, *Bombyx mori*.
472 *Heredity*. 2013;111(3):182-8.
- 473 16. Denell RE, Hummels KR, Wakimoto BT, Kaufman TC. Developmental studies
474 of lethality associated with the *Antennapedia* gene complex in *Drosophila*
475 *melanogaster*. *Dev Biol*. 1981;81(1):43-50.

- 476 17. Wakimoto BT, Kaufman TC. Analysis of larval segmentation in lethal genotypes
477 associated with the antennapedia gene complex in *Drosophila melanogaster*. *Dev.*
478 *Biol.* 1981;81(1):51-64.
- 479 18. Mizoguchi A, Ohashi Y, Hosoda K, Ishibashi J, Kataoka H. Developmental
480 profile of the changes in the prothoracicotropic hormone titer in hemolymph of the
481 silkworm *Bombyx mori*: correlation with ecdysteroid secretion. *Insect Biochem Mol*
482 *Biol.* 2001;31(4):349-58.
- 483 19. Fujiwara H, Hojyo T. Developmental profiles of wing imaginal discs of
484 flügellos(fl), a wingless mutant of the silkworm, *Bombyx mori*. *Genes Evol.*
485 1997;207(1):12-8.
- 486 20. D'Avino PP, Thummel CS. The ecdysone regulatory pathway controls wing
487 morphogenesis and integrin expression during *Drosophila* metamorphosis. *Dev. Biol.*
488 2000;220(2):211-24.
- 489 21. Schubiger M, Truman JW. The RXR ortholog USP suppresses early metamorphic
490 processes in *Drosophila* in the absence of ecdysteroids. *Development*
491 2000;127(6):1151-9.
- 492 22. Kawasaki H, Kiguchi K, Agui N, Iwashita Y. Ecdysteroid titer and Wing
493 Development during the Pupal-Adult Transformation of *Bombyx mori*. *ZOOL Sci.*
494 1986;3:301-8.
- 495 23. Futahashi R, Okamoto S, Kawasaki H, Zhong YS, Iwanaga M, Mita K, et al.
496 Genome-wide identification of cuticular protein genes in the silkworm, *Bombyx mori*.
497 *Insect Biochem Mol Biol.* 2008;38(12):1138-46.
- 498 24. Riddiford LM, Cherbas P, Truman JW. Ecdysone receptors and their biological
499 actions. *Vitam Horm.* 2000;60:1-73.
- 500 25. Petryk A, Warren JT, Marques G, Jarcho MP, Gilbert LI, Kahler J, et al. Shade is
501 the *Drosophila* P450 enzyme that mediates the hydroxylation of ecdysone to the
502 steroid insect molting hormone 20-hydroxyecdysone. *Proc. Natl. Acad. Sci. USA.*
503 2003;100(24):13773-8.
- 504 26. Wang HB, Moriyama M, Iwanaga M, Kawasaki H. Ecdysone directly and
505 indirectly regulates a cuticle protein gene, *BMWCP10*, in the wing disc of *Bombyx*
506 *mori*. *Insect Biochem Mol Biol.* 2010;40(6):453-459.
- 507 27. Cifuentes FJ, Garcíabellido A. Proximo-distal specification in the wing disc of
508 *Drosophila* by the nubbin gene. *Proc. Natl. Acad. Sci. USA.* 1997;94(21):11405-10.
- 509 28. Matsuoka Y, Monteiro A. Hox genes are essential for the development of
510 eyespots in *Bicyclus anynana* butterflies. *Genetics.* 2021;217(1):1-9.
- 511 29. Hombría CG. Butterfly eyespot serial homology: enter the Hox genes. *BMC Biol.*
512 2011;9:26.
- 513 30. Rewitz KF, Rybczynski R, Warren JT, Gilbert LI. Developmental expression of
514 *Manduca* shade, the P450 mediating the final step in molting hormone synthesis. *Mol*
515 *Cell Endocrinol.* 2006;247(1-2):166-74.
- 516 31. Shahin R, Iwanaga M, Kawasaki H. Expression profiles of cuticular protein genes
517 in wing tissues during pupal to adult stages and the deduced adult cuticular structure
518 of *Bombyx mori*. *Gene.* 2018;646:181-194.
- 519 32. Gilbert LI, Warren JT. A molecular genetic approach to the biosynthesis of the

- 520 insect steroid molting hormone. *Vitam Horm.* 2005;73:31-57.
- 521 33. Monier B, Astier M, Sémériva M, Perrin L. Steroid-dependent modification of
522 Hox function drives myocyte reprogramming in the *Drosophila* heart. *Development.*
523 2005;132(23):5283-93.
- 524 34. Ou J, Deng HM, Zheng SC, Huang LH, Feng QL, Liu L. Transcriptomic analysis
525 of developmental features of *Bombyx mori* wing disc during metamorphosis. *BMC*
526 *Genomics.* 2014;15(1):820.
- 527
- 528

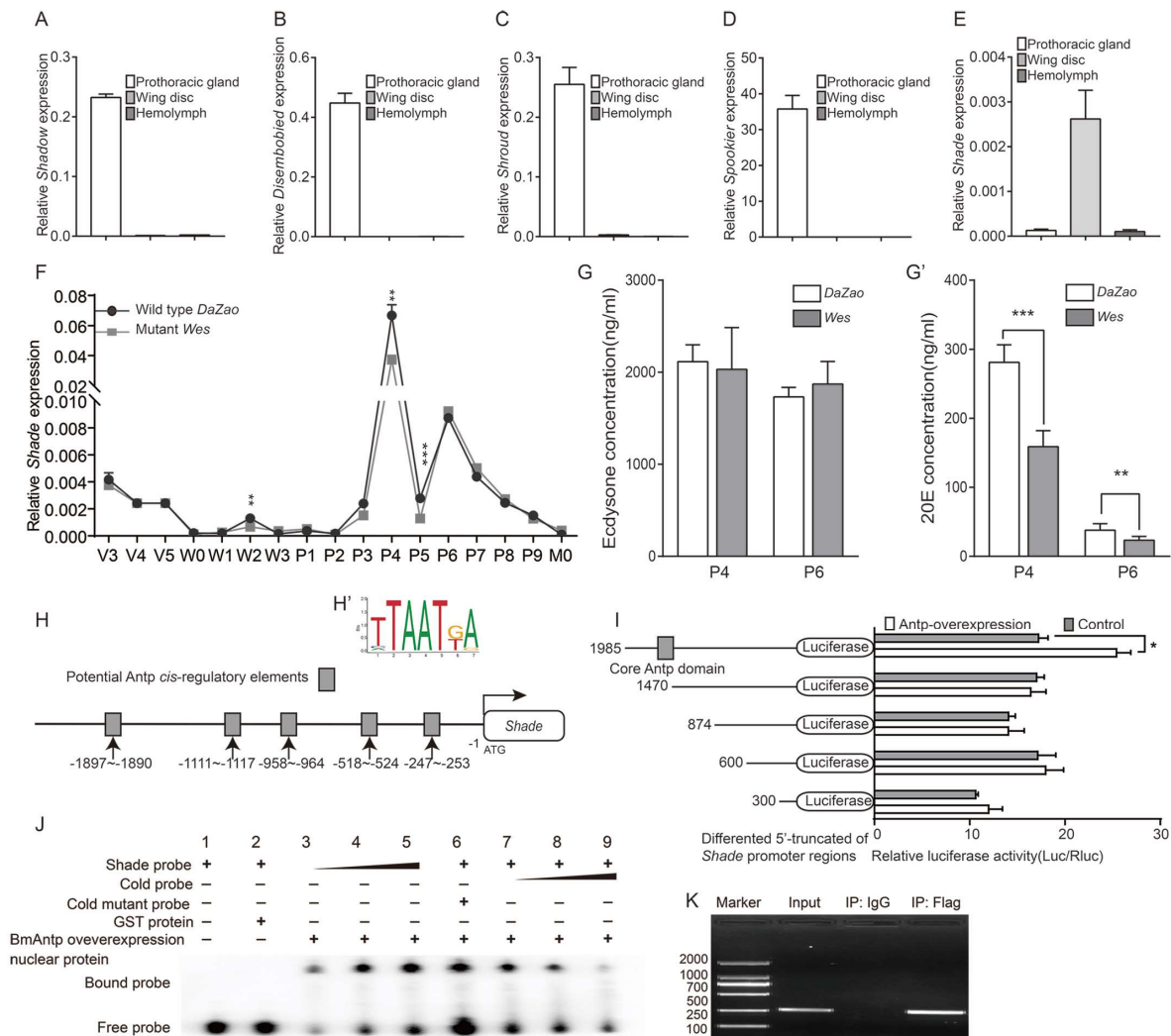
529 **Figure Captions**



530

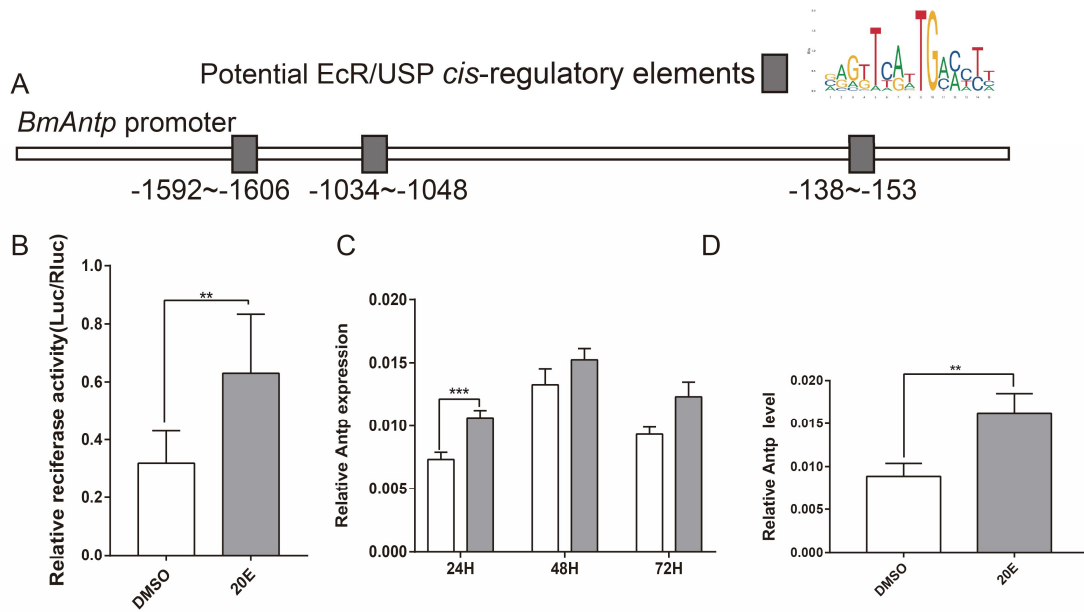
531 **Fig 1. *Antp* is essential for wing development in *B. mori*.** (A) Temporal expression pattern of *Antp* in wild-type (*DaZao*) forewing and

532 hindwing discs by qRT-PCR. (B) Expression profiles of *Antp* in the wing discs of wild-type and mutant (*Wes*) lines from larvae to adult stages.
533 (C) Phenotype of the wing discs in wild-type *DaZao* and *Wes* (*Antp*^{+/-}) mutants over different time points. (D) Relative *Antp* expression levels of
534 dsRNA-treated larvae at 24 h, 48 h, and 72 h after dsRNA treatments. Animals injected with ds*EGFP* served as controls. (E) Wing phenotype of
535 dsRNA-treated silkworm adults. (F) Genomic structure of *Antp*. The single guide RNA (sgRNA) target sequence is in black font and the
536 protospacer adjacent motif (PAM) sequence is in red font. The red arrows mark the sgRNA targets on the *Antp* gene. F and R indicate the
537 approximate locations of the amplification primers. (G) Representative phenotypes of wild-type (top) and mutated (bottom) insects, with smaller
538 and abnormal wings. (H) Mutated sequences of crispr individuals. The wild-type sequence, showed above the mutant sequences, is in black
539 and the PAM sequence is in red font. The size of indels is shown to the right of the sequence. Inserted sequenced are in green font. For all graphs,
540 V is the 5th instar larvae, V1–V7 means days 1–7 of the 5th instar larvae; W is the wandering larval stage, W0–W3 indicates days 0–3 of the
541 wandering larval stage; P, the pupal stage, P0–P9 indicates days of 0–9 of the pupal stage; M0, newly emerged adult. All experimental data
542 shown are means ± SE (n=3). Asterisks indicate significant differences with a two-tailed t-test: *P < 0.05, **P < 0.01, ***P < 0.001.



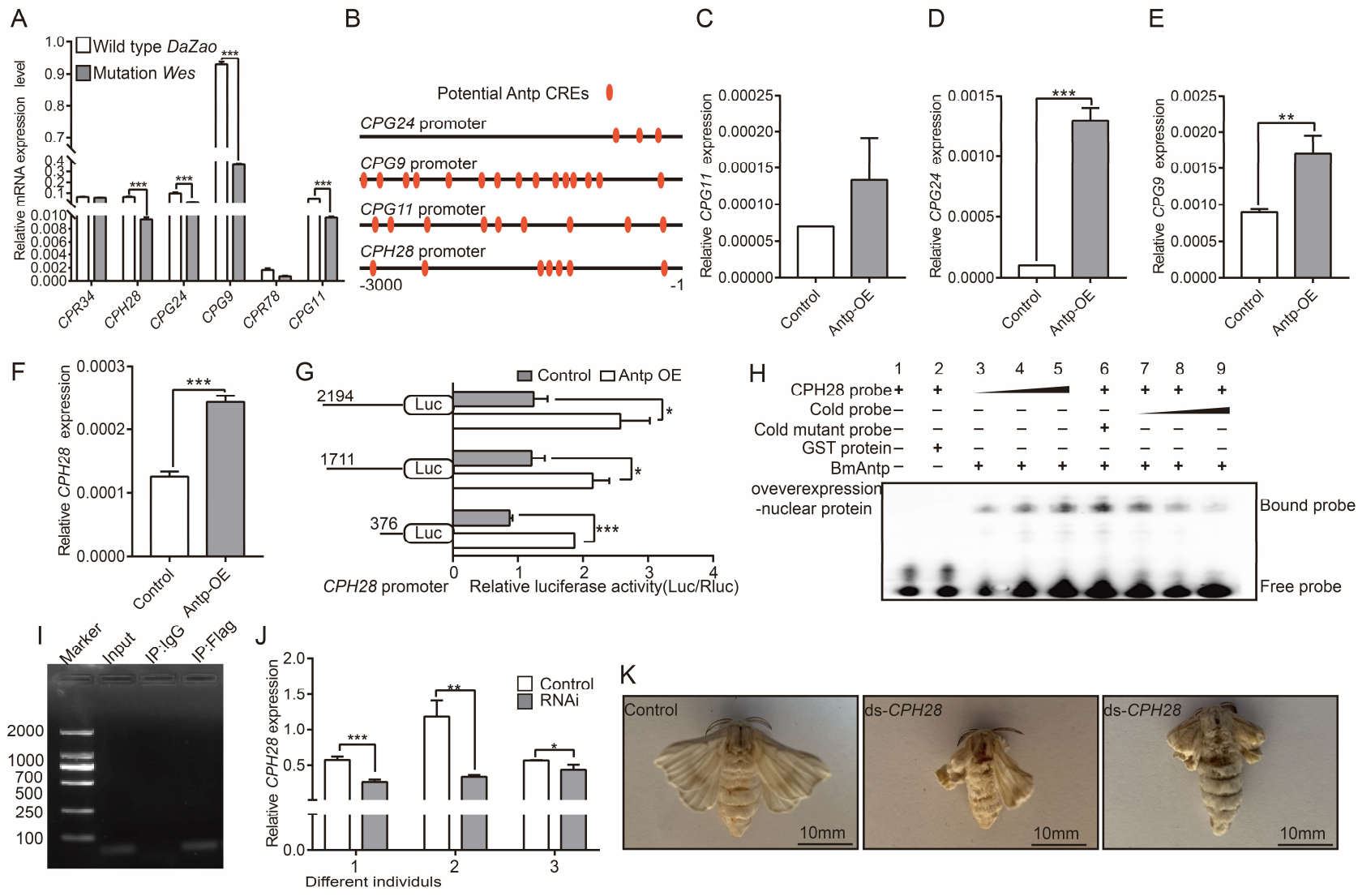
543 **Fig 2. *Antp* induces 20E synthesis in the wing tissue by directly binding to the**
544 ***shade* promoter. (A–E)** Relative expression of five ecdysteroid enzyme genes in the
545 prothoracic gland, hemolymph, and wing disc. (F) mRNA levels of *shade* were
546 detected by qRT-PCR from the 5th instar larval stage to the adult stage. (G and G')
547 The titers of ecdysone (G) and 20E (G') in *Bombyx* wing discs of WT *DaZao* and *Wes*
548 mutants (*Antp*^{+/-}) at P4 and P6. (H) Location of the five potential Antp binding sites in
549 the *shade* promoter. (H') Classic Antp binding motif. (I) The effect of different
550 truncations of the *shade* promoter on luciferase activity when Antp is overexpressed
551 in BmN cells. (J) EMSA confirmed that the recombinant Antp proteins bind to the nt
552 -1897--1890 region in the *Shade* promoter. Coincubating nucleoproteins from
553 *Escherichia coli* strain BL21 (DE3) competent cells overexpressing GST with labeled
554 Antp probes resulted in loss of the binding band. Purified recombinant BmAntp
555 protein could bind to the biotinylated probes in a dose-dependent manner (lanes 3–5),
556 and this binding could be competitively suppressed by unlabeled probe (lane 6). The
557 unlabeled probe with mutation in the core-binding motif of BmAntp could not
558 compete for BmAntp binding to biotinylated probes (lanes 7–9). We further validated
559 the direct regulation of BmAntp on *shade* transcription through in vivo ChIP-PCR
560 following the BmN cells which were overexpression of FLAG-tagged BmAntp. (K)

561 ChIP-PCR assay of the direct binding of Antp to the *shade* promoter in BmN cells
562 with Antp-Flag overexpression. Specific primers covering Antp binding sites of the 3
563 *Shade* promoter were used. Comparing with nonspecific IgG antibody, used as a
564 negative control, the antibody against FLAG can specifically immunoprecipitate the
565 DNA regions including -1985 to -1470 of the Shade promoter. All experimental data
566 shown are means \pm SE (n=3). Asterisks indicate significant differences with a
567 two-tailed t-test: *P < 0.05, **P < 0.01, and ***P < 0.001.
568

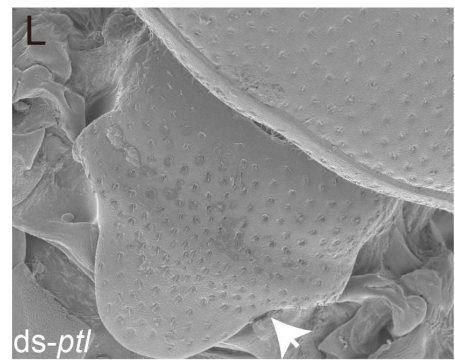
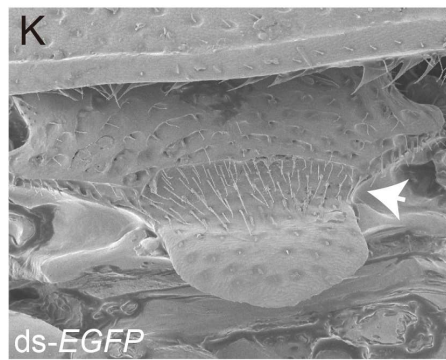
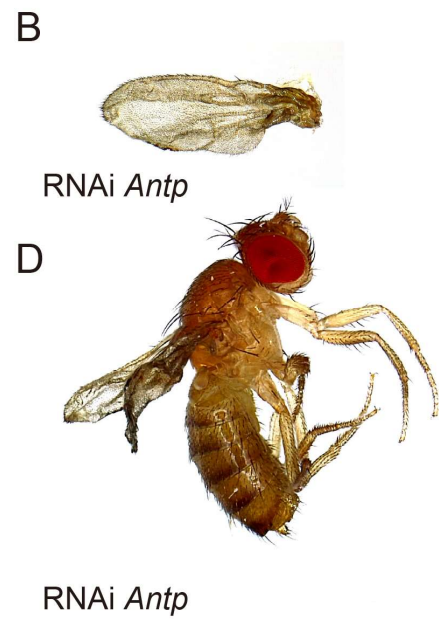
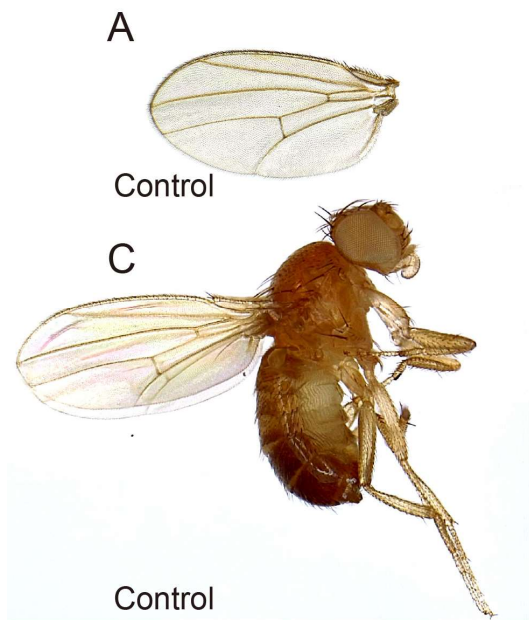


569

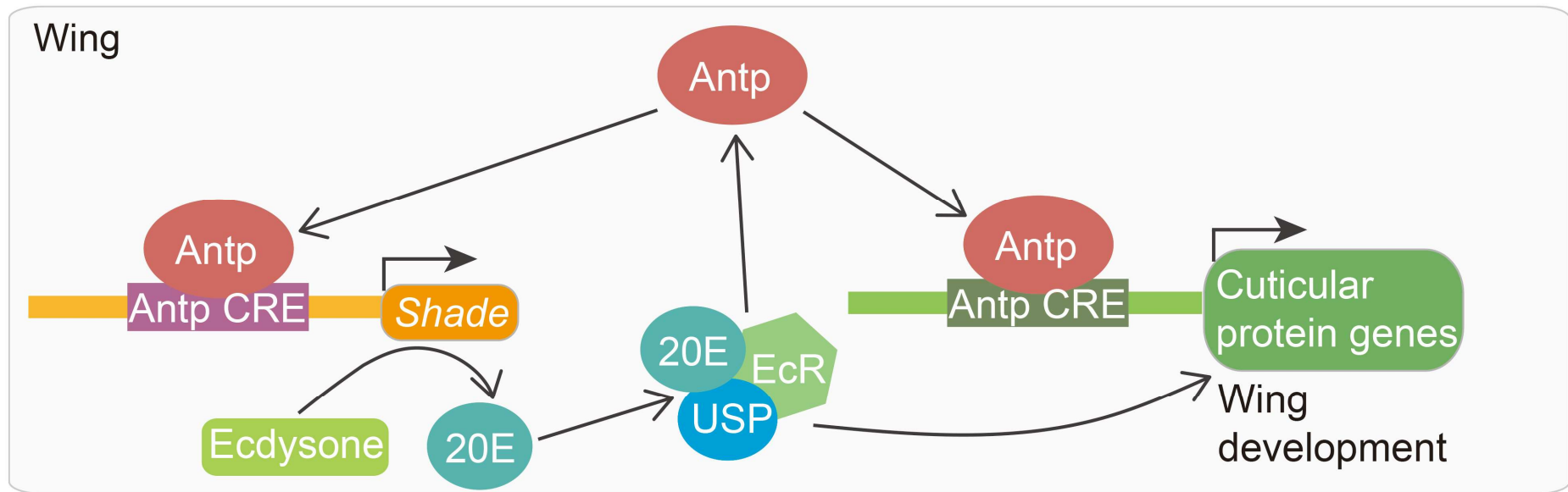
570 **Fig 3. 20E induced expression of *Antp*.** (A) Location of potential *Antp* binding sites
571 in the *Antp* promoter. (B) Effects of 20E treatment on the luciferase activity driven by
572 the *Antp* promoter. (C and D) Levels of *Antp* expression increase in BmN cells (C)
573 and wing discs (D) after 20E treatment. All of the experimental data shown are
574 means \pm SE (n=3). Asterisks indicate significant differences with a two-tailed t-test:
575 **P < 0.01.



577 **Fig 4. *Antp* regulates the expression of cuticular protein genes essential for wing development.** (A) mRNA levels of cuticular protein genes
578 in wing discs of *DaZao* and *Wes* (*Antp*^{+/-}) at P5. (B) Schematic of the potential *Antp* CREs in the promoters of cuticular protein genes. (C–F)
579 Relative cuticular protein genes expression detected in *Antp* overexpression BmN cells. (G) *Antp* increased luciferase activity driven by different
580 truncations of the *CPH28* promoter. (H) Electrophoretic mobility shift assay (EMSA) of the binding nuclear proteins extracted from
581 *Antp*-overexpressing *Escherichia coli* strain BL21 (DE3) competent cells with the *Antp* binding motif. Co-incubating nucleoproteins from *E.*
582 *coli* strain BL21 (DE3) competent cells overexpressing glutathione S-transferase (GST) with labeled *Antp* probes results in loss of the binding
583 band. The binding signal between recombinant GST-Bm*Antp* protein and *Antp* binding motif probe was gradually enhanced with increased
584 probe levels (lanes 3–5). (I) ChIP-PCR assay shows that *Antp* binds directly to *Antp* binding motifs present in the *CPH28* promoter in BmN cells.
585 A Flag tag was fused to Bm*Antp* and an anti-Flag tag antibody was used in the ChIP assay. The cells were transfected with recombinant plasmid
586 Flag-Bm*Antp*, and then the cells were collected for ChIP assay 48 h post-transfection. The results showed that the anti-Flag antibodies, but not
587 IgG (a negative control), precipitated DNA containing the *Antp* binding motifs in the cells transfected with the Flag-Bm*Antp* expressing plasmid.
588 (J) qPCR analyses of *CPH28* expression in wing discs of different individuals, 48 h after knock down of *CPH28* and of a control sequence
589 (containing the scrambled siRNA sequence). (K) Comparisons of adult wing morphology after dsRNA injections. All experimental data shown
590 are means ± SE (n=3). Asterisks indicate significant differences with a two-tailed t-test: *P < 0.05, **P < 0.01, and ***P < 0.001.
591



593 **Fig 5. *Antp* is essential for wing development in *Drosophila* and *Tribolium*.** (A and B) Adult *Drosophila* wings from control (A) and *Antp*
 594 RNAi (B) treated individuals. (C and D) Adult *Drosophila* of control (C) and *Antp* RNAi (D) treated individuals. (E and F) *ptl* RNAi leads to
 595 reduction of elytra and hindwings in *Tribolium* adults. (E) ds-*EGFP*. (F) ds-*ptl*. (G and I) The elytron (G) and hindwing (I) from a ds-*EGFP*
 596 treated individual. (H and J) The elytron (H) and hindwing (J) from a ds-*ptl* treated individual. (K and L) *ptl* RNAi leads to a uniform
 597 mesonotum (white arrow in K and L). (K) ds-*EGFP*. (L) ds-*ptl*.



598
 599 **Fig 6. Proposed model on how *Antp* regulates wing development in *B. mori*.** The Hox gene *Antp* plays an essential role in wing development.
 600 It does this by directly enhancing transcription of the steroidogenic enzyme gene *shade* in wings and, thus, controlling the synthesis of an
 601 essential growth hormone, 20E, directly in the wing tissue. In turn 20E signaling upregulates *Antp* expression. *Antp* also directly regulates the
 602 expression of critical cuticular protein genes in both forewings and hindwings.